

# LEARNING FIRST-TO-SPIKE POLICIES FOR NEUROMORPHIC CONTROL USING POLICY GRADIENTS

*Bleema Rosenfeld, Osvaldo Simeone, and Bipin Rajendran*

Department of Electrical and Computer Engineering  
New Jersey Institute of Technology, Newark, NJ 07102, USA

## ABSTRACT

Artificial Neural Networks (ANNs) are currently being used as function approximators in many state-of-the-art Reinforcement Learning (RL) algorithms. Spiking Neural Networks (SNNs) have been shown to drastically reduce the energy consumption of ANNs by encoding information in sparse temporal binary spike streams, hence emulating the communication mechanism of biological neurons. In this work, the use of SNNs as stochastic policies is explored under an energy-efficient first-to-spike action rule, whereby the action taken by the RL agent is determined by the occurrence of the first spike among the output neurons. A policy gradient-based algorithm is derived and implemented on a windy grid-world problem. Experimental results demonstrate the capability of SNNs as stochastic policies to gracefully trade energy consumption, as measured by the number of spikes, and control performance.

**Index Terms**— Spiking Neural Network, Reinforcement Learning, Policy Gradient, Neuromorphic Computing.

## 1. INTRODUCTION

Artificial neural networks (ANNs) are currently being used as parameterized non-linear models that serve as inductive bias for a large number of machine learning tasks, including notable applications of Reinforcement Learning (RL) to control problems [1]. While ANNs rely on clocked floating-point operations on real numbers, Spiking Neural Networks (SNNs) are more closely modeled on biological neurons, and are emerging as an energy-efficient alternative backed by major technology companies, including IBM and Intel [2, 3]. Applications of SNNs, and of associated neuromorphic hardware solutions, to supervised, unsupervised, and RL problems have been reported in a number of works, first in the computational neuroscience literature and more recently in the context of machine learning [4, 5, 6].

Two key problems in the design of SNN-based solutions for learning tasks are the encoding of the input data into a spike-domain format suitable for processing by an SNN, and the decoding the spiking output of an SNN into the output space of interest, e.g., the action space of an RL agent. For encoding, standard solutions include rate and time encoding [7]. For decoding in a finite discrete space, rate decoding is typically considered, whereby the output neuron with the larger spike count is assumed to identify the SNN’s decision [8, 9]. Furthermore, SNN models can be broadly classified as *deterministic*, such as the leaky integrate-and-fire model [7] and *probabilistic*, such as the Generalized Linear Model (GLM) [10].

Prior work on RL using SNNs as policy or action-value function approximators has by and large adopted deterministic SNN models and rate decoding, under either rate encoding [11, 12], or time encoding [13]. However, most papers have relied on learning rules based on versions of reward modulated STDP as defined in [14], with the possible inclusion of eligibility traces for each synapse in order to deal with delayed rewards [15]. The policy gradient algorithm was studied in [16]. An exception to the discussed focus on deterministic models is [12], which maps in an approximate fashion the operation of a (probabilistic) Boltzmann machine to that of an SNN to estimate the action-value function.

In all of the reviewed studies, exploration is made possible by a range of mechanisms such as  $\epsilon$ -greedy in [15] and stochasticity introduced at the synaptic level [12, 16], requiring the addition of some external source of randomness. In contrast, in this paper, we investigate the use of probabilistic SNN policies that naturally enable exploration thanks to the inherent randomness of their decisions, hence making it possible to learn while acting in an on-policy fashion. We note that reference [11] discusses the addition of noise to a deterministic SNN model to induce exploration of the state space from a hardware perspective.

---

O. Simeone is on leave from NJIT. This research was supported in part by the European Research Council (ERC) under the European Unions Horizon 2020 Research and Innovation Program (Grant Agreement No. 725731) and the U.S. National Science Foundation through grants 1525629 and 1710009.

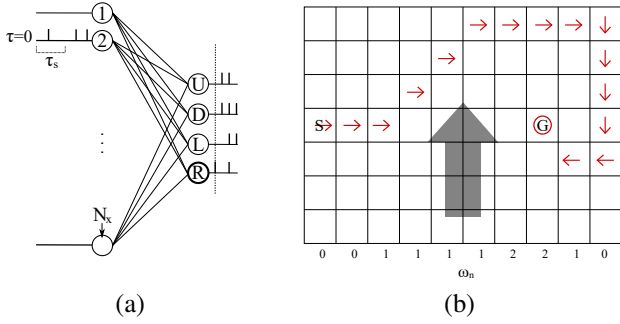


**Fig. 1.** (a) SNN first-to-spike policy with action selected (R in the illustration) among Up, Down, Left, and Right marked with a bold line and decision time marked with a dashed vertical line; (b) An example of a realization of an action sequence in a windy grid-world problem.

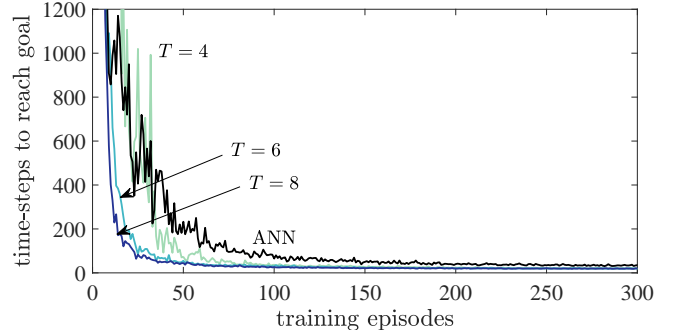


**Fig. 2.** Number of time-steps needed to reach the goal state as a function of the training episodes.

Due to an SNN’s event-driven activity, its energy consumption depends mostly on the number of spikes that are output by its neurons. This is because the idle energy consumption of neuromorphic chips is generally extremely low (see, e.g., [17]). With this observation in mind, this work proposes the use of a probabilistic SNN, based on GLM spiking neurons, as a stochastic policy that operates according to a first-to-spike decoding rule. The rule outputs a decision as soon as the first output neuron outputs a spike, as illustrated in Fig. 1(a), hence potentially reducing energy consumption. A gradient-based updating rule is derived that leverages the analytical tractability of the first-to-spike decision criterion under the GLM model (see also [18] for an application to a supervised learning classification algorithm).

The rest of the paper is organized as follows. Sec. 2 describes the problem formulation and the GLM-based SNN model. Sec. 3 introduces the proposed policy gradient on-policy learning rule. Experiments and discussions are reported in Sec. 5.

## 2. PROBLEM DEFINITION AND MODELS

**Problem definition.** We consider a standard RL single-agent problem formulated on the basis of discrete-time Markov Decision Processes (MDPs). Accordingly, at every time-step  $t = 1, 2, \dots$ , the RL agent takes an action  $A_t$  from a finite set of options based on its knowledge of the current environment state  $S_t$  with the aim of maximizing a long-term performance criterion. The agent’s policy  $\pi(A|S, \theta)$  is a parameterized probabilistic mapping from the state space to the action space, where  $\theta$  is the vector of trainable parameters. After taking an action  $A_t$ , the agent receives a numeric reward  $R_{t+1}$  and the environment transitions to a new state  $S_{t+1}$ , where both  $R_{t+1}$  and  $S_{t+1}$  are generally random functions of the action  $A_t$  and state  $S_t$  with unknown conditional probability distributions.

An episode, starting at time  $t = 0$  in some state  $S_0$ , ends at time  $t^G$ , when the agent reaches a goal state  $S^G$ . The performance of the agent’s policy  $\pi$  is measured by the long-term discounted average reward

$$V_\pi(S_0) = \sum_{t=0}^{\infty} \gamma^t \mathbf{E}_\pi[R_t], \quad (1)$$

where  $\gamma < 1$  is a discount factor. The reward  $R_t$  is assumed to be zero for all times  $t > t^G$ . With a proper definition of the reward signal  $R_t$ , this formulation ensures that the agent is incentivized to reach the terminal state in as few time-steps as possible.

While the approach proposed in this work can apply to arbitrary RL problems with discrete finite action space, we will focus on a standard windy grid-world environment [19]. Accordingly, as seen in Fig. 1(b), the state space is an  $M \times N$  grid of positions and the action space is the set of allowed horizontal and vertical single-position moves, i.e., Up, Down, Left, or Right. The start state  $S_0$  and the terminal state  $S^G$  are fixed but unknown to the agent. Each column  $n = 1, \dots, N$  in the grid is subject to some unknown degree of ‘wind’, which pushes the agent upward by  $\omega_n$  spaces when it moves from a location in that column. The reward signal is defined as  $R_{t+1} > 0$  if  $S_{t+1} = S^G$  and, otherwise, we have  $R_{t+1} = 0$ .

**Probabilistic SNN model.** In order to model the policy  $\pi(A|S, \theta)$ , as we will detail in the next section, we adopt a probabilistic SNN model. Here we briefly review the operation of GLM spiking neurons [10]. Spiking neurons operate over

---

**Algorithm 1:** Policy Gradient Rule for First-to-Spike (FtS) SNNs

---

**Input:** randomly initialized parameter  $\theta$ , learning rate  $\eta_i$ ,  $i = 1, 2, \dots$

```
1  $i = 1$ 
2 repeat
3   while  $S_t \neq S^G$  do
4     encode  $S_t$  in spike domain
5     run SNN and set  $A_t \leftarrow$  index of FtS neuron
6     observe next state and reward  $S_{t+1}, R_{t+1}$ 
7   end
8    $V_{t^G+1} = 0$ 
9   for  $t=t^G : -1 : 1$  do
10     $V_t = R_{t+1} + \gamma V_{t+1}$ 
11     $\theta \leftarrow \theta + \eta_i \nabla_{\theta} \log \pi(A_t|S_t, \theta) V_t$ 
12  end
13   $i \leftarrow i + 1$ 
14 until convergence
```

---

discrete time  $\tau = 1, \dots, T$  and output either a “0” or a “1” value at each time, where the latter represents a spike. We emphasize that, as it will be further discussed in the next section, the notion of time  $\tau$  for a spiking neuron is distinct from the time axis  $t$  over which the agent operates. Consider a GLM neuron  $j$  connected to  $N_s$  pre-synaptic (input) neurons. At each time instant  $\tau = 1, \dots, T$  of the neuron’s operation, the probability of an output spike at neuron  $j$  is given as  $\sigma(u_{j,\tau})$ , where  $\sigma(x) = 1/(1 + \exp(-x))$  is the sigmoid function and  $u_{j,\tau}$  is the neuron’s membrane potential

$$u_{j,\tau} = \sum_{i=1}^{N_s} \alpha_{i,j}^{\dagger} x_{i,\tau-\tau_s:\tau-1} + b_j. \quad (2)$$

In (2), the  $\tau_s \times 1$  vector  $\alpha_{i,j}$  is the so called *synaptic kernel* which describes the operation of the synapse from neuron  $i$  to neuron  $j$ ;  $b_j$  is a bias parameter; and  $x_{i,\tau-\tau_s:\tau-1}$  collects the past  $\tau_s$  samples of the  $i$ th input neuron. As in [10], we model the synaptic kernel as a linear combination  $\alpha_{i,j} = B w_{i,j}$  of  $K_s$  basis functions, described by the columns of  $\tau_s \times K_s$  matrix  $B$ , with the  $K_s \times 1$  weight vector  $w_{i,j}$ . We specifically adopt the raised cosine basis functions in [10].

### 3. POLICY-GRADIENT LEARNING USING FIRST-TO-SPIKE SNN RULE

In this section, we propose an on-policy learning algorithm for RL that uses a first-to-spike SNN as a stochastic random policy. Although the approach can be generalized, we focus here on the fully connected two-layer SNN shown in Fig. 1(a). In the SNN, the first layer of neurons encode the current state of the agent  $S_t$ , as detailed below, while there is one output GLM neuron for each possible action  $A_t$  of the agent, with  $N_s = N_x$  inputs. For example, in the grid world of Fig. 1(b), there are four output neurons. The policy  $\pi(A|S, \theta)$  is parameterized by the vector  $\theta$  of synaptic weights  $\{w_{i,j}\}$  and biases  $\{b_j\}$  for all the output neurons as defined in (2). We now describe encoding, decoding, and learning rule.

**Encoding.** A position  $S_t$  is encoded into  $N_x$  spike trains, i.e., binary sequences, with duration  $T$  samples, each of which is assigned to one of the neurons in the input layer of the SNN. We emphasize that the time duration  $T$  is internal to the operation of the SNN, and the agent remains at time-step  $t$  while waiting for the outcome of the SNN. In order to explore the trade-off between encoding complexity and accuracy, we partition the grid into  $N_x$  sections, or windows, each of size  $W \times W$ . Each section is encoded by one input neuron, so that increasing  $W$  yields a smaller SNN at the cost of a reduced resolution of state encoding. Each position  $S_t$  on the grid can be described in terms of the index  $s(S_t) \in \{1, \dots, N_x\}$  of the section it belongs to, and the index  $w(S_t) \in \{1, \dots, W^2\}$  indicating the location within the section using left-to-right and top-to-bottom ordering. Accordingly, using rate encoding, the input to the  $j$ th neuron is an i.i.d. spike train with probability of a spike given by  $p_j = p_{\min} + ((p_{\max} - p_{\min})/(W^2 - 1)) (w(S_t) - 1)$  if  $j = s(S_t)$  and  $p_j = 0$  otherwise, for given parameters  $p_{\min}, p_{\max} \in [0, 1]$  and  $p_{\max} \geq p_{\min}$ .

**Decoding.** We adopt a first-to-spike decoding protocol, so that the output of the SNN directly acts as a stochastic policy, inherently sampling from the policy  $\pi(A|S, \theta)$  induced by the first-to-spike rule. If no output neuron spikes during the input presentation time  $T$ , no action is taken, while if multiple output neurons spike concurrently, an action is chosen from among them at random.

Given the synaptic weights and biases in vector  $\theta$ , the probability that the  $j$ th output neuron spikes first, and thus the probability that the network chooses action  $A = j$ , is given as  $\Pr(A = j) = \sum_{\tau=1}^T p_{\tau}(j)$ , where

$$p_{\tau}(j) = \prod_{k \neq j, \tau'=1}^{\tau} (1 - \sigma(u_{k, \tau'})) \sigma(u_{j, \tau}) \prod_{\tau'=1}^{\tau-1} (1 - \sigma(u_{j, \tau'})) \quad (3)$$

is the probability that the  $j$ th output neuron spikes first at time  $\tau$ , while the other neurons do not spike until time  $\tau$  included.

**Policy-gradient learning.** After an episode is generated by following the first-to-spike policy, the parameters  $\theta$  are updated using the policy gradient method [19]. The gradient of the objective function (1) equals

$$\nabla_{\theta} V_{\pi}(S_0) = \mathbb{E}_{\pi}[V_t \nabla_{\theta} \log \pi(A_t | S_t, \theta)], \quad (4)$$

where  $V_t = \sum_{t'=t}^{\infty} \gamma^{t'} R_{t'}$  is the discounted return from the current time-step until the end of the episode and the expectation is taken with respect to the distribution of states and actions under policy  $\pi$  (see [19, Ch. 13]). The gradient in (4) can be computed as [18]

$$\nabla_{w_{i,k}} \log \pi_{\theta}(A_t = j | S_t, \theta) = \begin{cases} -\sum_{\tau=1}^T h_{\tau} \sigma(u_{k, \tau}) B^T x_{i, \tau - \tau_s : \tau - 1} & k \neq j \\ -\sum_{\tau=1}^T (h_{\tau} \sigma(u_{j, \tau}) - q_{\tau}) B^T x_{i, \tau - \tau_s : \tau - 1} & k = j, \end{cases} \quad (5)$$

and

$$\nabla_{b_k} \log \pi_{\theta}(A_t = j | S_t, \theta) = \begin{cases} -\sum_{\tau=1}^T h_{\tau} \sigma(u_{k, \tau}) & k \neq j \\ -\sum_{\tau=1}^T h_{\tau} \sigma(u_{j, \tau}) - q_{\tau} & k = j \end{cases} \quad (6)$$

where

$$h_{\tau} = \sum_{\tau'=\tau}^T q_{\tau'}, \text{ and } q_{\tau} = \frac{p_{\tau}}{\sum_{\tau=1}^T p_{\tau}}.$$

The first-to-spike policy gradient algorithm is summarized in Table 1, where the gradient (4) is approximated using Monte-Carlo sampling in each episode [19 Ch. 5].

#### 4. RESULTS AND DISCUSSION

In this section, we provide numerical results for the grid world example described in Sec. 2 with  $M = 7$ ,  $N = 10$ ,  $S_0$  and  $S^G$  at positions (4,1) and (4,8) on the grid respectively, ‘wind’ level per columns defined by the values  $\omega_n$  indicated in Fig. 1(b), and  $K_{s=\tau_s}$  for all simulations. Throughout, we set  $p_{\min} = 0.5$  and  $p_{\max} = 1$  for encoding in the spike domain and a learning schedule,  $\eta_i = (\eta_{i-1}) / (1 - k(i-1))$  with  $\eta_0 = 10^{-2}$ . Training is done for 25 epochs of 1000 iterations each, with 500 test episodes to evaluate the performance of the policy after each epoch. We compare the performance of an SNN trained as discussed with that of an ANN with the same two-layer architecture and number of input and output neurons with a soft-max output layer. In order to keep the set-up consistent across the ANN and SNN solutions, the input to each input neuron  $i$  of the ANN is given by the probability value, or spiking rate,  $p_i$  defined in Sec. 3, and the ANN is trained via standard policy gradient [19] using the parameters mentioned above. Note that, unlike the SNN, the ANN requires an external random number generator to output a decision with probabilities determined by the soft-max layer (see also [20]).

We start by considering the convergence of the learning process along the training episodes in terms of number of time-steps to reach the goal state. In Fig. 2, we plot the performance, averaged over the 25 training epochs, of the SNN policy with different values of input presentation duration  $T$  and GLM parameters  $K_{s=\tau_s} = 4$ , as well as that of the reference ANN, both using encoding window size  $W = 1$ , and hence  $N_x = 70$  input neurons. The SNN policy is seen to learn more quickly how to reach the goal point in fewer time-steps as  $T$  is increased. This improvement stems from the proportional increase in the number of input spikes that can be processed by the SNN, enhancing the accuracy of input encoding. It is also interesting to observe that the ANN policy is outperformed by the SNN policy. This is due to the capability of SNNs to carry out temporal processing by means of the synaptic kernel. The latter is learned through the  $K_s$  synaptic weights, which contrast with the single synaptic weight of ANNs.

The previous experiment used maximum resolution input encoding, assigning an individual neuron to each grid location. In order to analyze the scalability of the algorithm to cases in which such a complex representation is not plausible, we now consider coarser state encodings by increasing the encoding window size  $W$ . The window size  $W$  also offers a useful handle on the network spatial complexity in terms of the number of input neurons and synapses. Fig. 3 plots the number of time-steps to reach the goal (top) and the total number of spikes per input sample across the network or spike frequency (bottom), as a function of the number of input neurons for different values of  $T$  and synaptic memory  $\tau_s$ . These quantities are averaged over the test episodes. It is seen that, as long as the window size is no larger than  $W = 4$ , no significant increase of time-steps

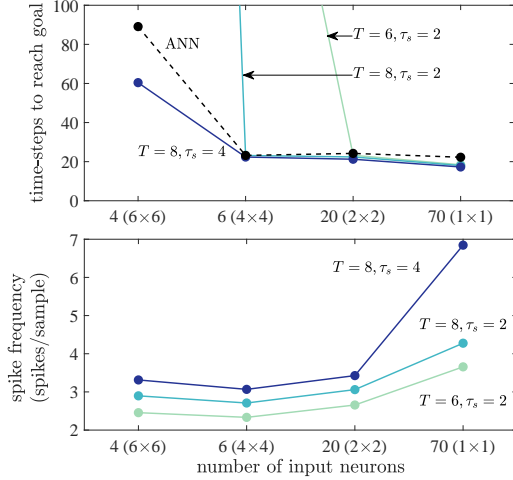


**Fig. 3.** Average number of time-steps to reach goal (top) and average number of total spikes per sample (bottom) in the test episodes as a function of the number of input neurons  $N_x$  (also indicated is the size of the  $W \times W$  encoding window).

to reach the goal is incurred. Furthermore, a better resolution, i.e., a smaller  $W$ , can enhance the performance gains of the SNN over the ANN. Interestingly, this improved performance is obtained with a spike frequency that increases only gradually despite the larger number of input neurons. This can be seen as a result of accelerated decision making thanks to the first-to-spike decision rule.

While the previous figure referred to the performance over the test episodes after learning, we finally investigate how the spike frequency varies over the training episodes in Fig. 4. The initially very low spike frequency can be interpreted as an exploration phase, where the network makes mostly random action choices by largely neglecting the input spikes. After the first hundred episodes, the SNN slows decision making by increasingly relying on the observation of a larger number of input spikes. Finally, the spike frequency is decreased since the network can optimize its synaptic kernels so that it needs only a short input presentation time before making a decision.

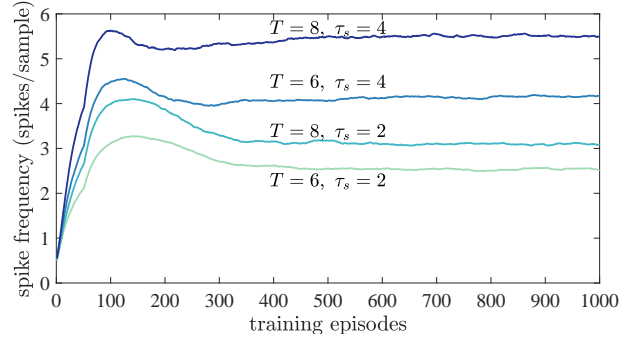


**Fig. 4.** Average spike frequency over the training episodes for the SNN policy.

## 5. REFERENCES

- [1] Max Jaderberg, Wojciech M Czarnecki, Iain Dunning, Luke Marris, Guy Lever, Antonio Garcia Castaneda, Charles Beattie, Neil C Rabinowitz, Ari S Morcos, Avraham Ruderman, et al., “Human-level performance in first-person multiplayer games with population-based deep reinforcement learning,” *arXiv preprint arXiv:1807.01281*, 2018.
- [2] Filipp Akopyan, Jun Sawada, Andrew Cassidy, Rodrigo Alvarez-Icaza, John Arthur, Paul Merolla, Nabil Imam, Yutaka Nakamura, Pallab Datta, Gi-Joon Nam, et al., “Truenorth: Design and tool flow of a 65 mw 1 million neuron programmable neurosynaptic chip,” *IEEE Transactions on Computer-Aided Design of Integrated Circuits and Systems*, vol. 34, no. 10, pp. 1537–1557, 2015.
- [3] Mike Davies, Narayan Srinivasa, Tsung-Han Lin, Gautham Chinya, Yongqiang Cao, Sri Harsha Choday, Georgios Dimou, Prasad Joshi, Nabil Imam, Shweta Jain, et al., “Loihi: A neuromorphic manycore processor with on-chip learning,” *IEEE Micro*, vol. 38, no. 1, pp. 82–99, 2018.
- [4] Danilo J Rezende, Daan Wierstra, and Wulfram Gerstner, “Variational learning for recurrent spiking networks,” in *Advances in Neural Information Processing Systems*, 2011, pp. 136–144.
- [5] David Kappel, Robert Legenstein, Stefan Habenschuss, Michael Hsieh, and Wolfgang Maass, “A dynamic connectome supports the emergence of stable computational function of neural circuits through reward-based learning,” *eNeuro*, vol. 5, no. 2, pp. ENEURO–0301, 2018.

- [6] Yingyezhe Jin, Peng Li, and Wenrui Zhang, “Hybrid macro/micro level backpropagation for training deep spiking neural networks,” *arXiv preprint arXiv:1805.07866*, 2018.
- [7] Wulfram Gerstner and Werner M Kistler, *Spiking neuron models: Single neurons, populations, plasticity*, Cambridge university press, 2002.
- [8] Jinling Wang, Ammar Belatreche, Liam Maguire, and Thomas Martin Mcginnity, “An online supervised learning method for spiking neural networks with adaptive structure,” *Neurocomputing*, vol. 144, pp. 526–536, 2014.
- [9] Nan Zheng and Pinaki Mazumder, “Online supervised learning for hardware-based multilayer spiking neural networks through the modulation of weight-dependent spike-timing-dependent plasticity,” *IEEE Transactions on Neural Networks and Learning Systems*, 2017.
- [10] Jonathan W Pillow, Liam Paninski, Valerie J Uzzell, Eero P Simoncelli, and EJ Chichilnisky, “Prediction and decoding of retinal ganglion cell responses with a probabilistic spiking model,” *Journal of Neuroscience*, vol. 25, no. 47, pp. 11003–11013, 2005.
- [11] Nan Zheng and Pinaki Mazumder, “Hardware-friendly actor-critic reinforcement learning through modulation of spike-timing-dependent plasticity,” *IEEE Transactions on Computers*, vol. 66, no. 2, pp. 299–311, 2017.
- [12] Takashi Nakano, Makoto Otsuka, Junichiro Yoshimoto, and Kenji Doya, “A spiking neural network model of model-free reinforcement learning with high-dimensional sensory input and perceptual ambiguity,” *PloS one*, vol. 10, no. 3, pp. e0115620, 2015.
- [13] Zhenshan Bing, Claus Meschede, Kai Huang, Guang Chen, Florian Rohrbein, Mahmoud Akl, and Alois Knoll, “End to end learning of spiking neural network based on r-stdp for a lane keeping vehicle,” in *2018 IEEE International Conference on Robotics and Automation (ICRA)*. IEEE, 2018, pp. 1–8.
- [14] Răzvan V Florian, “Reinforcement learning through modulation of spike-timing-dependent synaptic plasticity,” *Neural Computation*, vol. 19, no. 6, pp. 1468–1502, 2007.
- [15] Myung Seok Shim and Peng Li, “Biologically inspired reinforcement learning for mobile robot collision avoidance,” in *Neural Networks (IJCNN), 2017 International Joint Conference on*. IEEE, 2017, pp. 3098–3105.
- [16] Eleni Vasilaki, Nicolas Frémaux, Robert Urbanczik, Walter Senn, and Wulfram Gerstner, “Spike-based reinforcement learning in continuous state and action space: when policy gradient methods fail,” *PLoS computational biology*, vol. 5, no. 12, pp. e1000586, 2009.
- [17] Catherine D Schuman, Thomas E Potok, Robert M Patton, J Douglas Birdwell, Mark E Dean, Garrett S Rose, and James S Plank, “A survey of neuromorphic computing and neural networks in hardware,” *arXiv preprint arXiv:1705.06963*, 2017.
- [18] Alireza Bagheri, Osvaldo Simeone, and Bipin Rajendran, “Training probabilistic spiking neural networks with first-to-spike decoding,” *arXiv preprint arXiv:1710.10704*, 2017.
- [19] Richard S Sutton and Andrew G Barto, *Reinforcement learning: An introduction*, MIT press, 2018.
- [20] Meire Fortunato, Mohammad Gheshlaghi Azar, Bilal Piot, Jacob Menick, Ian Osband, Alex Graves, Vlad Mnih, Remi Munos, Demis Hassabis, Olivier Pietquin, et al., “Noisy networks for exploration,” *arXiv preprint arXiv:1706.10295*, 2017.